PROCEEDINGS B

royalsocietypublishing.org/journal/rspb

Research

Cite this article: Schmidt FN *et al*. 2018 Ultra-high matrix mineralization of sperm whale auditory ossicles facilitates high sound pressure and high-frequency underwater hearing. *Proc. R. Soc. B* **285**: 20181820. http://dx.doi.org/10.1098/rspb.2018.1820

Received: 13 August 2018
Accepted: 20 November 2018

Subject Category:
Ecology

Subject Areas:
biomaterials, biomechanics, ecology

Keywords:
sperm whale, bone, biomaterial, matrix mineralization, quantitative backscattered electron imaging, Fourier-transform infrared spectroscopy

Author for correspondence:
Tim Rolvien
e-mail: t.rolvien@uke.de

Electronic supplementary material is available online at https://dx.doi.org/10.6084/m9.figshare.c.4320833.

THE ROYAL SOCIETY PUBLISHING

Ultra-high matrix mineralization of sperm whale auditory ossicles facilitates high sound pressure and high-frequency underwater hearing

Felix N. Schmidt[1], Maximilian M. Delsmann[1], Kathrin Mletzko[1], Timur A. Yorgan[1], Michael Hahn[1], Ursula Siebert[2], Björn Busse[1], Ralf Oheim[1], Michael Amling[1] and Tim Rolvien[1,3]

[1]Department of Osteology and Biomechanics, University Medical Center Hamburg-Eppendorf, Lottestrasse 59, 22529 Hamburg, Germany
[2]Institute for Terrestrial and Aquatic Wildlife Research, University of Veterinary Medicine Hannover, Foundation, Werftstrasse 6, 25761 Buesum, Germany
[3]Department of Orthopedics, University Medical Center Hamburg-Eppendorf, Martinistrasse 52, 20246 Hamburg, Germany

TR, 0000-0003-1058-1307

The auditory ossicles—malleus, incus and stapes—are the smallest bones in mammalian bodies and enable stable sound transmission to the inner ear. Sperm whales are one of the deepest diving aquatic mammals that produce and perceive sounds with extreme loudness greater than 180 dB and frequencies higher than 30 kHz. Therefore, it is of major interest to decipher the microstructural basis for these unparalleled hearing abilities. Using a suite of high-resolution imaging techniques, we reveal that auditory ossicles of sperm whales are highly functional, featuring an ultra-high matrix mineralization that is higher than their teeth. On a micro-morphological and cellular level, this was associated with osteonal structures and osteocyte lacunar occlusions through calcified nanospherites (i.e. micropetrosis), while the bones were characterized by a higher hardness compared to a vertebral bone of the same animals as well as to human auditory ossicles. We propose that the ultra-high mineralization facilitates the unique hearing ability of sperm whales. High matrix mineralization represents an evolutionary conserved or convergent adaptation to middle ear sound transmission.

1. Background

The middle ear's major function is to amplify sound vibrations before entering the fluid-filled cochlea. Terrestrial mammals have to overcome large acoustic impedance differences between air (low acoustic impedance) and inner ear fluid (high acoustic impedance), which are partly compensated by a tympanic membrane and sound transmission via the auditory ossicles. Impedance differences are reversed and in general much smaller in aquatic mammals such as whales [1] and the tympanic membrane is therefore not needed for hearing purposes [2]. Instead, whales have a highly mineralized tympanoperiotic complex containing the middle ear [1]. While being firmly fixed to the skull in baleen whales (mysticetes) [3,4], the tympanoperiotic complex is acoustically isolated from the skull to hinder direct osseous sound transmission in toothed whales (odontocetes) [3]. In toothed whales, the sound reaches the mandibular wall and is guided through the mandibular fat pad to the lateral tympanic bone (i.e. the tympanic plate) causing it to vibrate [1,5]. While low frequencies are also transmitted via head regions close to the external auditory meatus (skull vibrations), the mandibular 'sound route' is especially suited for high-frequency hearing (pressure load) [1]. This vibration caused by higher frequencies is achieved because of a high

impedance mismatch between the mandibular fat pad and the tympanic bone as well as the thinness of the tympanic plate [5]. The sound is then transmitted to the auditory ossicles; malleus, incus and stapes that have been found to be of dense compact bone [3,6]. A high mineralization of bone was found to be of major importance for sound perception as supported by an 86% mineralization of the tympanic bulla with an impressively high Young's modulus [7,8] resulting from mineralization and causing high impedance (a rough approximation of the impedance in case of a wave hitting a material in orthogonal direction can be written by the following equation: $Z = \sqrt{\rho \cdot E}$; where $Z =$ impedance, $\rho =$ density of a material and $E =$ Young's modulus of a material referring to [7]).

Sperm whales (*Physeter macrocephalus, Linnaeus, 1758)* are one of the deepest diving toothed whales that produce sounds with extreme loudness greater than 180 dB re 1 µPa, have exceptional frequency discrimination abilities and an estimated best hearing sensitivity from 0.1 to 30 kHz with frequencies of 2–4 and 10–16 kHz close to maximum energy [9,10]. In general, hearing frequencies in whales may go up to 120 kHz and more [2,10]. The high-frequency hearing of toothed whale (odontocete) species has been found to be limited by the bone mass of the auditory ossicles [11].

In humans, the auditory ossicles show signs of premature bone ageing including high bone matrix mineralization, osteocyte death and low bone remodelling [12,13], which is most probably needed for stable sound transmission throughout life. Compositional changes of auditory ossicles through specific gene mutations have been linked to conductive hearing loss in mice [14,15]. Therefore, the in-depth characterization of the auditory ossicles of mammals with exceptional hearing abilities and potential unique compositional features (i.e. sperm whales) is of major interest.

We have extracted the auditory ossicles of three sperm whales and performed a multiscale, high-resolution skeletal analysis in order to uncover the in-depth ossicular morphology and bone quality of one of the potentially hardest bone materials that is seen among the animal kingdom. Our results may provide further insights into the function of the whale's middle ear especially in relation to high-frequency hearing associated with echolocation.

2. Material and methods

(a) Specimens

The auditory ossicles were taken from three sperm whales of 12, 13 and 15 years of age [16,17]. All specimens were transferred with special documentation of no commercial or trading interests according to the environmental authority of Schleswig-Holstein (Germany) and approved by the Institute for Terrestrial and Aquatic Wildlife Research (ITAW) on behalf of the Schleswig-Holstein Wadden Sea National Park.

(b) High-resolution quantitative computed tomography and radiography

The tympanoperiotic complex of the sperm whales was scanned via high-resolution quantitative computed tomography (HR-pQCT) (Xtreme-CT®, Scanco Medical, Bruettisellen, Switzerland) at 60 kV/900 µA and a resolution of 82 µm as described previously [18]. Subsequently, the auditory ossicles were prepared and scanned using a digital radiography device at 45 kV for 5 s (Faxitron X-ray, Illinois, USA).

(c) Micro-computed tomography

To assess the gross morphology of all three auditory ossicles, they were isolated from the tympanoperiotic complex for micro-computed tomography (µ-CT) analysis using a water-cooled diamond band saw (Exakt, Norderstedt, Germany). µ-CT scanning was performed using a µ-CT42 (Scanco Medical AG, Brüttisellen, Switzerland) at 40 kV/114 mA with a voxel size of 10 µm as described [19]. Bone/tissue mineral density (TMD, mgHA cm^{-3}) was evaluated using the Scanco Micro-CT software.

For comparison, we have analysed the bones of human iliac crest and murine vertebral bones (wild-type C57BL/6 mice) as well as sperm whale vertebral bone regarding the bone mineral density (BMD) using bone specimens from previous studies and our archive [16,20] ($n \geq 3$ per group). Furthermore, the teeth of humans, mice and the same sperm whales were analysed ($n = 3$). Dentin and enamel were evaluated separately. Three incus specimens of three human relatively age-matched donors (age 21, 22, 23 years) were included from a previous study [13]. Lastly, the ossicles of wild-type mice were analysed ($n = 3$).

(d) Bone preparation, histology and quantitative backscattered electron microscopy

The µ-CT scanned ossicles were fixed in 3.7% phosphate buffered saline buffered formaldehyde for 7 days, dehydrated in an ascending ethanol series and embedded in a methylmethacrylate-based resin (Heraeus Kulzer, Technovit 7200 VLC, Wehrheim im Taunus, Germany). Subsequently, specimens were ground to 100 µm, and stained with toluidine blue [21]. Quantitative backscattered electron imaging (qBEI) was performed to assess the bone mineral density distribution (BMDD) as previously described [22–24]. Embedded incus and vertebral body specimens were polished and carbon coated for qBEI analyses. The scanning electron microscope (LEO 435 VP, LEO Electron Microscopy Ltd., Cambridge, England) was operated at 20 kV and 680 pA at a constant working distance of 20 mm (BSE Detector, Type 202, K.E. Developments Ltd., Cambridge, England). The grey values of the backscattered signal intensities correlate with the calcium content (weight-%) of bone [25]. The following parameters were evaluated using a custom-made Matlab routine: mean calcium concentration (CaMean, wt%), most frequent calcium concentration (CaPeak, wt%) and standard deviation of the calcium distribution (CaWidth, wt%). The acquired images were thresholded using ImageJ software (ImageJ, 1.49v, National Institutes of Health, USA - imagej.nih.gov/ij/) and the osteocyte number (N.Ot/B.Ar, 1 mm^{-2}) and lacunar area (Lc.Ar, μm^2) were calculated from the images (200x magnification).

(e) Fourier-transform infrared spectroscopy

The incus samples (sperm whale and human) and vertebral body samples (sperm whale) were repolished after qBEI imaging to ensure no sputtering material to be on the surface. A Spotlight 400 System (PerkinElmer, Waltham, MA, USA) attached to a Frontier Spectroscope (PerkinElmer, Waltham, MA, USA) was used to measure the spectral maps. Attenuated total reflectance (ATR) mode was used and the crystal surface was placed to the surface of the bone specimens. After ensuring sufficient contact of the crystal to the surfaces, a scan of 64 × 64 pixels per specimen was conducted (pixel size = 6.25 µm, 12 scans per pixel). Automatic background subtraction was done using the distributers' software SpectrumImage (R.1.8.0.0410, PerkinElmer, Whattham, USA). After completing all scans automatic ATR correction and atmospheric correction was done using the same software. Further processing of the spectral maps was done on a customized Matlab (The MathWorks Inc., Natick, MA, USA) routine. Automated polymethylmethacrylate (PMMA) weighting and subtraction was integrated. To calculate the mineral to matrix ratio (MMR), the phosphate peak

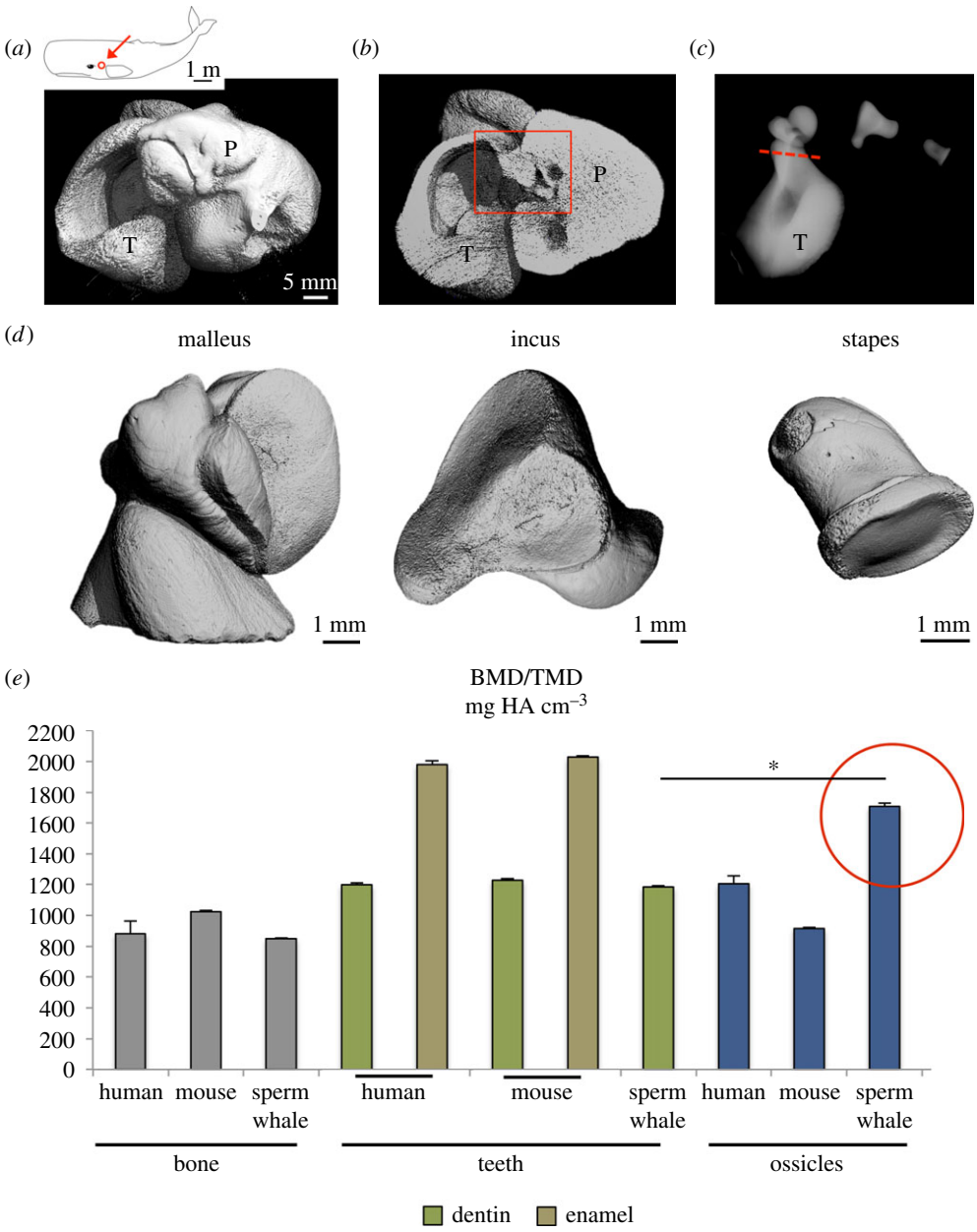

Figure 1. Overview of auditory ossicles in sperm whales and their ultra-high matrix mineralization among species. (*a*) 3D reconstruction of the tympano-periotic complex (T-P) using HR-pQCT. All specimens were obtained from the right side. (*b*) Virtual cut section identifies the auditory ossicles. (*c*) Contact radiography of the three ossicles. The red line indicates the plane where the malleus was separated from the tympanic bone. (*d*) 3D reconstructions of the malleus, incus and stapes using µ-CT to reveal highly intact and congruent joint surfaces of the ossicles. (*e*) An extensive comparative approach regarding the mineral density of different tissues showing the significantly higher mineralization of sperm whale auditory ossicles compared to their own vertebral bone and teeth as well as to bone and dentin of humans and mice. $*p < 0.05$.

(1154–900 cm^{-1}) was integrated and the area under the curve (AUC) was divided by the AUC of the integrated amide I peak (1710–1600 cm^{-1}). This calculation was performed in the same manner for the vertebral bodies, the human incus and the whale incus specimens. Additionally, the carbonate-to-phosphate ratio (CPR) was calculated integrating the carbonate peak (890–850 cm^{-1}) and dividing the AUC by the AUC of the phosphate peak. AUC has been calculated with one base-point for each peak at the lower of the two limits of each interval to ensure high sensitivity. Mean values were calculated for each map and averaged for each group and stated with standard deviation.

(f) Nano-indentation

Nano-indentation was carried out on an Agilent Nano Indenter G200 system (Agilent Technologies, Santa Clara, CA, USA) using a Berkovich tip. The specimens were polished and subsequently mounted on a platform with resin. The surface was approached at a speed of 10 nm s^{-1}. Depth limit was set to 2000 nm and strain rate target was 0.05 s^{-1}. Sixteen indents were placed in three standardized regions of each ossicle. In vertebral trabecular bone, eight indents were performed in two different trabeculae. Indents were subsequently imaged by electron microscopy (backscattered mode) to exclude the indents that hit PMMA. All valid indents per specimen were averaged calculating the mean hardness and Young's modulus (GPa).

(g) Statistical analysis

Statistical analysis was done using SPSS 22 (IBM, New York, USA). If comparing more than two groups an ANOVA was performed with Bonferroni as the *post hoc* test. Groups were not checked for a normal distribution for imaging methods owing to a sample size of three per group. For nano-indentation, a non-parametric Kruskal–Wallis test was used to examine significant differences using the adjusted significance owing to a non-normal distribution of the indents.

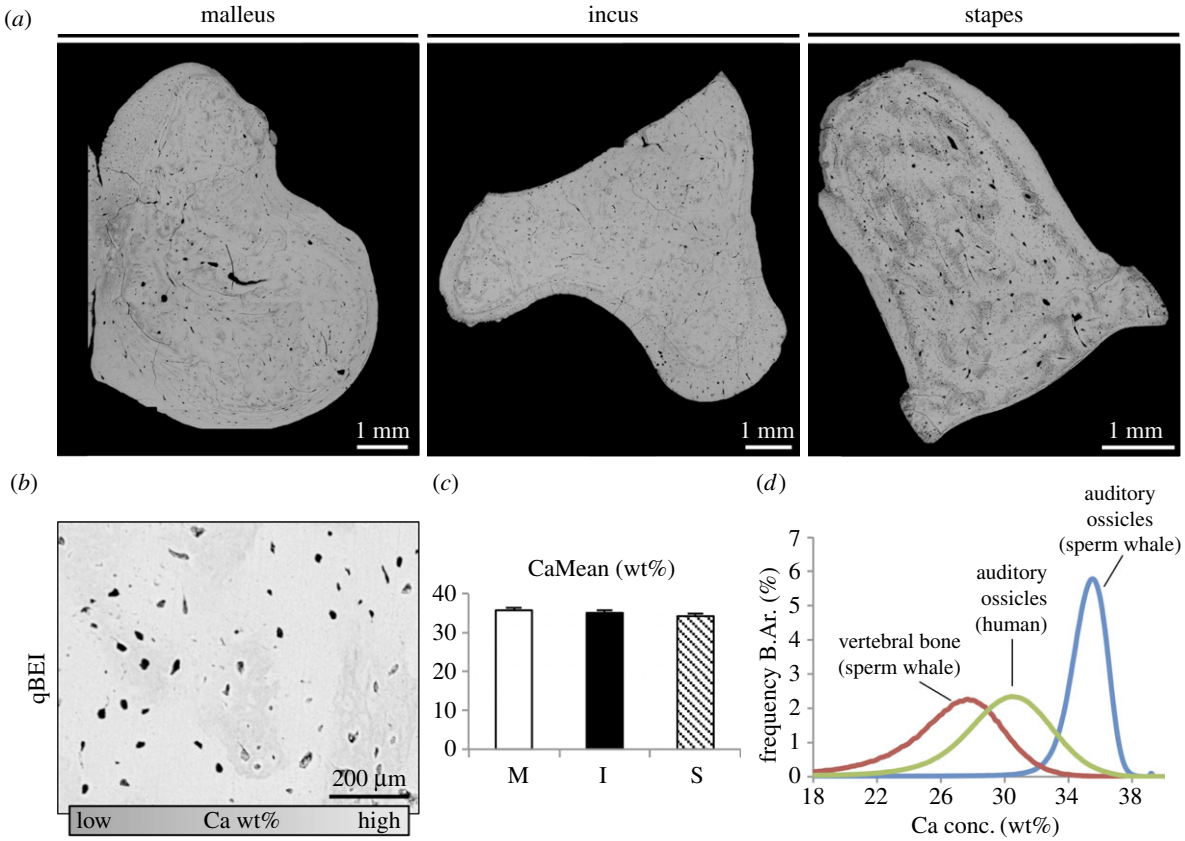

Figure 2. Quantitative backscattered electron imaging (qBEI) confirms the high matrix mineralization. (*a*) Overview images acquired by backscattered electron imaging. (*b*) qBEI revealed very high grey levels (bright) indicating a very high matrix mineralization. (*c*) Bar graph showing no difference in mineralization between the three ossicles. (*d*) Bone mineral density distribution analysis indicating a narrow peak of high mineralization in comparison to the sperm whale vertebral bone as well as human auditory ossicles.

3. Results

(a) Auditory ossicles of sperm whales are functional and highly mineralized compared to mineralized tissues of humans and mice

The auditory ossicles were located in the centre of the tympano-periotic complex as typically found in odontocete ears (figure 1*a*,*b*). While the incus and stapes could be separated without further sectioning, the malleus was cut from the thin tympanic lamella (figure 1*c*). µ-CT revealed that the three ossicles had perfectly congruent articular surfaces (figure 1*d*). BMD of the whale's incus was 1708 ± 21 mgHA cm^{-3}, indicating that the overall mineralization of these bones was significantly higher than their own vertebral bone as well as trabecular bone of humans and mice (figure 1*e*). Furthermore, the ossicles of sperm whales were also more highly mineralized than ossicles of humans and mice (both incus specimens). While tooth enamel of humans and mice was more highly mineralized, dentin was lower mineralized than the ossicles of sperm whales (figure 1*e*). We found that the overall mineralization of sperm whale teeth (enamel and dentin cannot be differentiated) was even lower than that of the auditory ossicles of the same animals (figure 1*e*).

(b) The ultra-high matrix mineralization is accompanied by nanospherite occlusions in osteocyte lacunae

Mineralization analysis using qBEI pointed to very high and homogeneous grey levels indicating an ultra-high matrix mineralization around 35 wt% and no significant differences between the three ossicles (figure 2*a*–*c*). When comparing the micro-morphological BMDD curves of sperm whale ossicles with their vertebrae as well as with auditory ossicles of humans, we detected a higher mineralized bone with a narrower mineralization distribution curve (i.e. lower heterogeneity) (figure 2*d*). Further imaging revealed an osteonal structure of all ossicles, which is typically found in cortical bone (figure 3*a*). While there was no significant difference in the osteocyte lacunar number between the three ossicles, the stapes featured significantly larger osteocyte lacunae (figure 3*b*,*c*). Detailed investigation of the osteocyte lacunae revealed a high number of osteocyte lacunae that were either completely mineralized or that showed an accumulation of calcified nanospherites (figure 3*d*). The number of mineralized lacunae per bone area was higher in the malleus and incus when compared with the stapes as well as when compared with human ossicles [13] (figure 3*e*). In the histological analysis of the ground sections, we identified various osteocyte lacunae with cell nuclei (indicating viable bone) and a connection of osteocytes via canaliculi with a different morphology than typically seen in humans or mice (i.e. branched morphology).

(c) The peculiar mineralization pattern leads to extremely high hardness

Fourier-transform infrared spectroscopy (FTIR) analysis revealed further detailed bone quality characteristics regarding the MMR (i.e. the amount of mineral per amount of

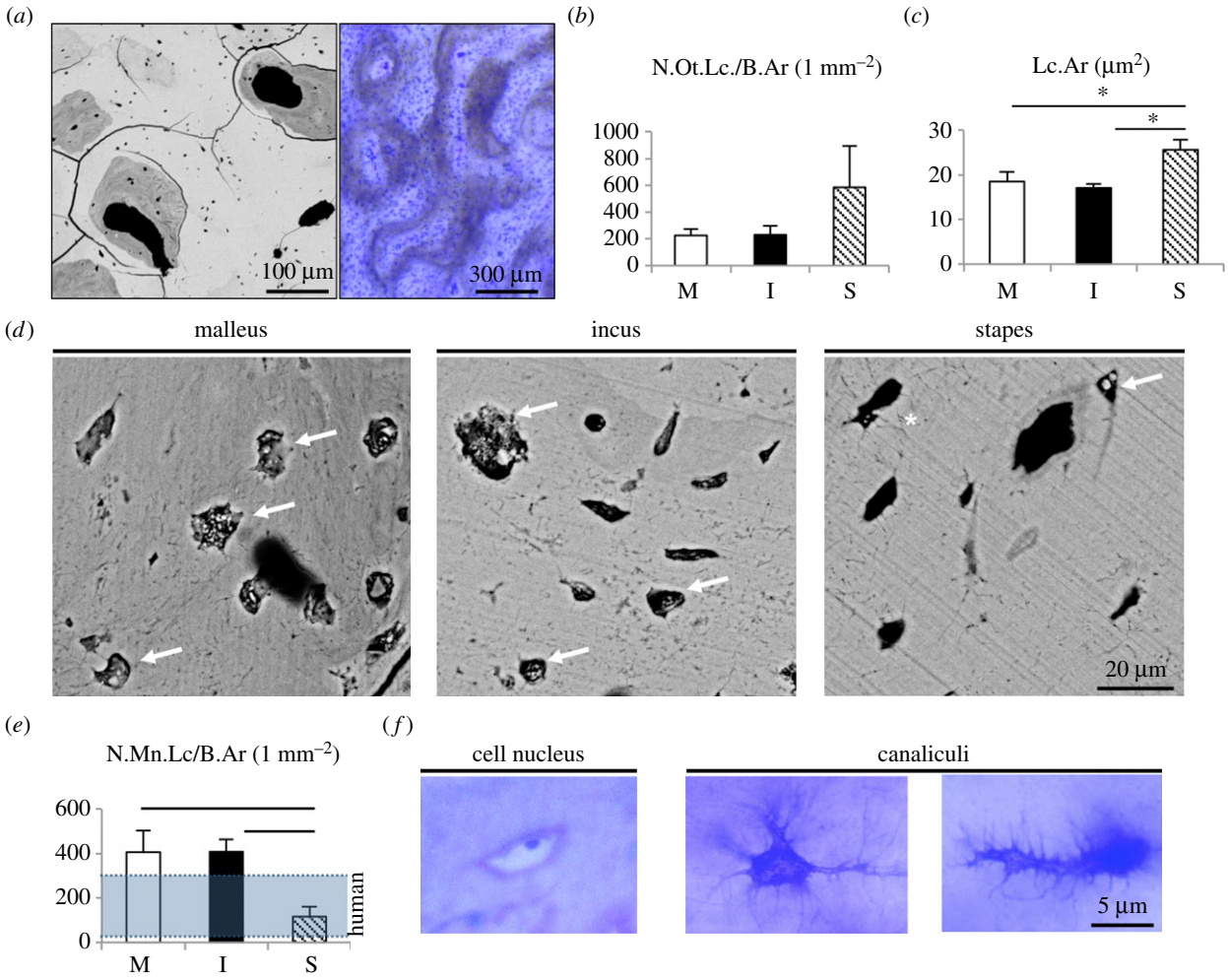

Figure 3. Osteocyte characteristics. (*a*) Left: Backscattered electron imaging of whale ossicular bone (not normalized to the grey values of qBEI) highlight osteonal structures. Lower brightness represents lower mineralization, differences in grey levels pointed to vital bone remodelling. Right: corresponding toluidine blue staining of a ground section. (*b*) The number of osteocyte lacunae per bone area was not different between malleus, incus and stapes. (*c*) In the stapes, osteocyte lacunae were enlarged compared to the malleus and incus. (*d*) Osteocyte lacunae were filled with calcified nanospherites (arrows). Asterisk: osteocyte canaliculi. (*e*) The number of mineralized lacunae was higher than in human auditory ossicles [13] in the malleus and incus and lower in the stapes. (*f*) Histology indicating viable osteocytes with cell nucleus (left) and branched-like osteocyte canaliculi (middle and right). *$p < 0.05$.

collagen) and the CPR (i.e. the mineral age) (figure 4*a*,*b*). The MMR and CPR values were calculated from the spectra (figure 4*c*). MMR was 3.9 times higher in whale ossicles compared to human ossicles (27.78 ± 0.28 versus 7.17 ± 1.04, $p < 0.001$). Furthermore, the vertebral trabecular bone of the same whales featured an MMR that was 5.31 times lower in the sperm whales than their ossicular bone (27.78 ± 0.28 versus 5.27 ± 1.04, $p < 0.001$) (figure 4*d*). CPR calculations showed a significantly higher ratio in whale ossicles compared to human ossicles (0.01513 ± 0.00091 versus 0.01067 ± 0.00067, $p < 0.001$). Compared to the vertebral bodies, the CPR was 1.85 times higher in the sperm whale ossicles ($p < 0.001$, figure 4*e*).

Nano-indentation was performed to determine the hardness of the whale ossicles. Indents were imaged by electron microscopy to confirm their localization within the bone (figure 5*a*). The analyses revealed that the sperm whale incus had a significantly higher Young's modulus than both whale vertebra and human incus (figure 5*b*). Furthermore, the bone was significantly harder compared to the vertebral bone as well when compared with human incus (figure 5*c*).

(d) The stapes of sperm whales is distinctly shaped

When investigating the stapes of sperm whales, we found that both crura were filled with osteonal bone as opposed to the stapes of humans and mice (figure 6*a*). Additional length measurements revealed that the stapes length was significantly lower to that of humans and mice in relation to body length and skull width (figure 6*b*,*c*), which indicates a possible negative allometric relationship between these parameters among the species. It has to be noted that skull width is most probably a better parameter for interpreting these relationships, given that sperm whales have an extremely large body length since their whole tail (caudal vertebrae) is included (although the tail was also included in length measurements in mice).

4. Discussion

In this study, we have demonstrated the unparalleled compositional aspects of a sperm whale's auditory ossicles that facilitate high sound pressure and high-frequency hearing by transmitting the auditory signal from the tympanic plate to the oval window. More specifically, a functional hypermineralization of ossicles is present and might represent an adaptation

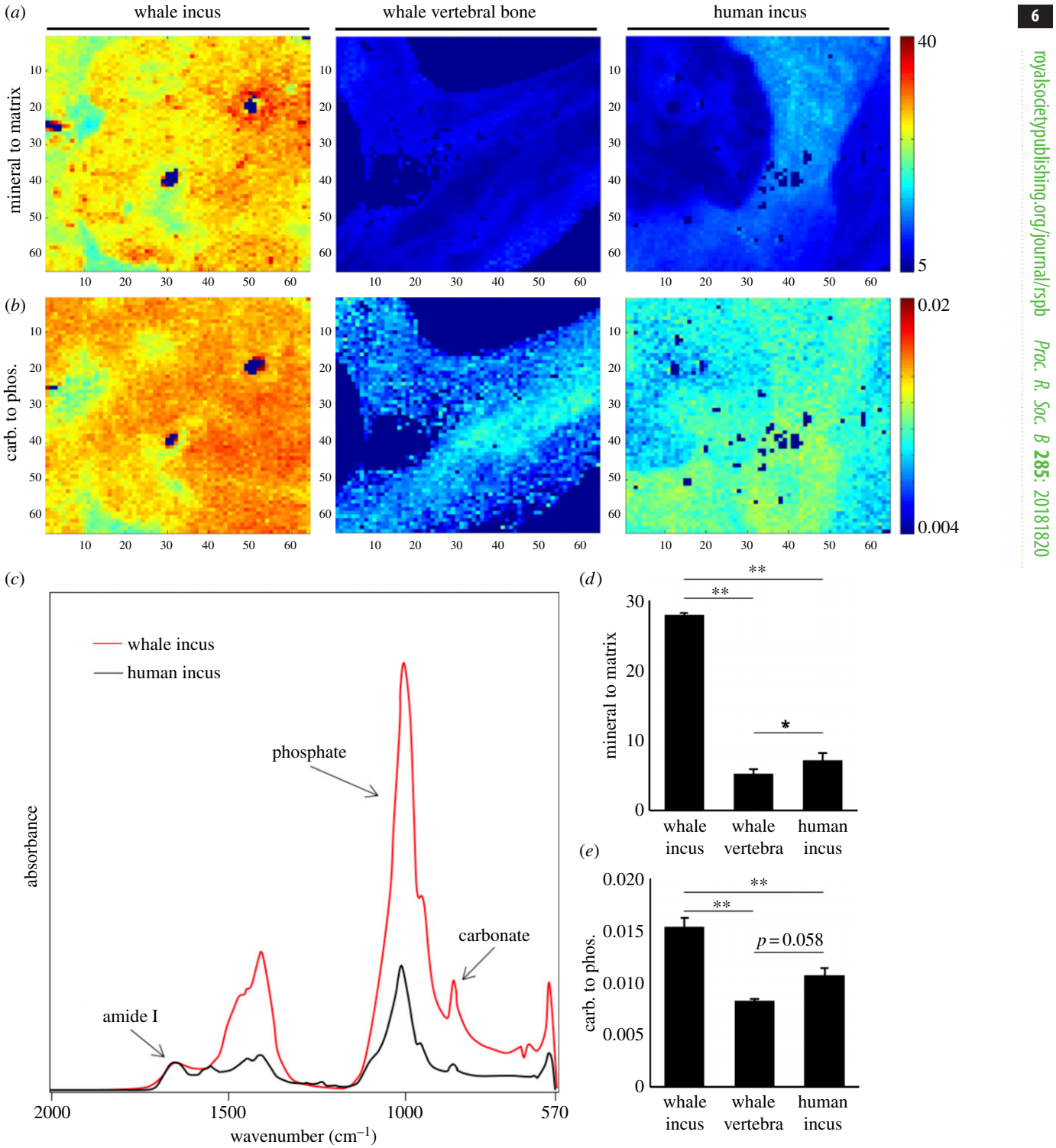

Figure 4. Compositional aspects of the ossicles using FTIR imaging. (*a*) Higher mineral to matrix ratio (MMR) in the whale incus compared to whale vertebral bone and human incus. Dark blue pixels are areas with high PMMA content that were excluded from the evaluation (*b*) Carbonate-to-phosphate ratio (CPR) is clearly elevated in sperm whale ossicles (left) compared to the other specimens, pixel size = 6.25 µm. (*c*) FTIR spectra of whale incus (red) and human incus. Clearly, a higher phosphate peak can be seen if taking the amide I peak to the same absorbance. Amide I peak represents the collagen content, the phosphate peak represents the mineral for MMR. (*d*) Differences in MMR and (*e*) CPR. *$p < 0.05$, **$p < 0.001$.

to the greatly different function of ossicles compared to other parts of the skeleton, where not only hardness and stiffness is needed but also toughness to dissipate energy [26]. The very high mineralization, going in hand with relatively low collagen content may reduce damping and increase stiffness with respect to the high-frequency hearing of the whale. It is interesting to note that the ossicles were even more highly mineralized than their teeth. This phenomenon is not present in humans or mice, where teeth (i.e. enamel) are more highly mineralized than the ossicles. Nonetheless, the high matrix mineralization of auditory ossicles compared to other bones is also present in humans or mice indicating evolutionary conservation or convergence. We have shown that in human ossicles there is a rapid increase in mineralization during the first years of life [13]. There is also no evidence for relevant postnatal growth of the cochlear structures or ear ossicles with individual shapes [13,17]. This suggests a very early adaptation of the ossicular bone to its function, which persists throughout life.

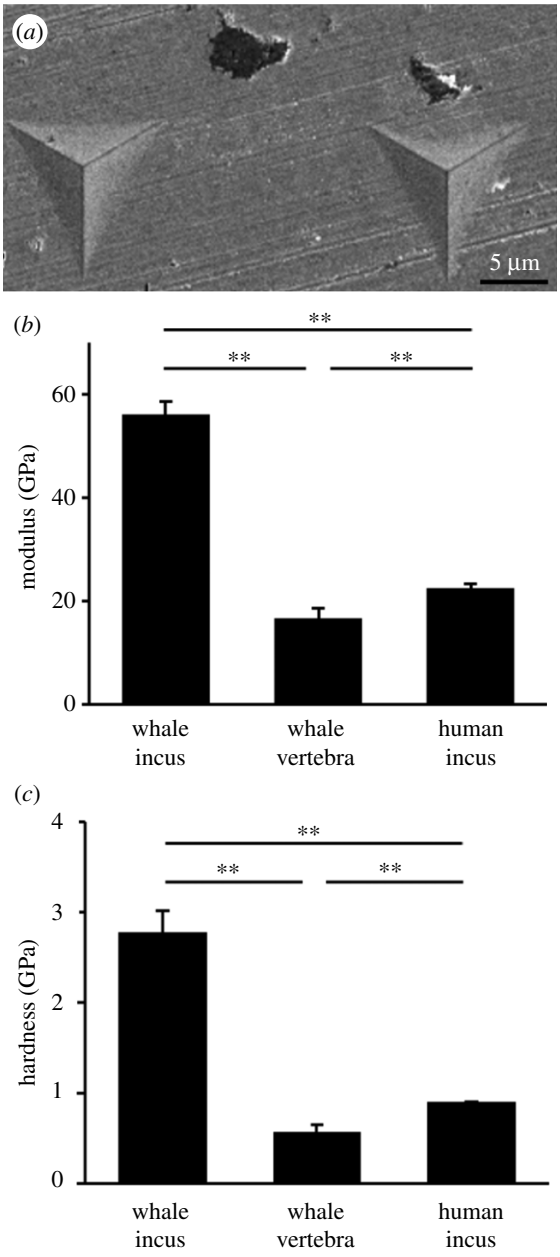

Figure 5. Increased microhardness detected by nano-indentation. (*a*) Indents were imaged with electron microscopy after the experiment to confirm correct position within bone, (*b*) modulus in GPa and (*c*) hardness in GPa. Both show a significantly higher value for whale ossicles than for both other groups. $^{**}p < 0.001$.

The high matrix mineralization was suggested to be crucial for optimal sound transmission throughout life [13]; however, the molecular mechanisms resulting in this high mineralization are unknown.

Early studies on whale tympanic bone [7,27] have shown a high mineralization and hardness in the tympanic bones, raising questions about material properties, composition and mineralization of sperm whale ossicles in relation to its frequency range of hearing as well as deep diving. Our analyses revealed equal mineralization of all three bones of the ossicular chain and an extraordinarily high mineralization of the ossicular bones compared to human auditory ossicles and the same whales' vertebral bodies as well as teeth. These results are in line with results found in other whale species [6] and the high mineralization of the connected tympanic bone. The functional hypermineralization of the ossicles is especially noteworthy in comparison with the vertebral bodies, which are loaded structures of the whale with a need for toughness and deformability. In ossicles, a high mineralization is needed to reduce an impedance mismatch, which also exists between water and normally mineralized bone [7]. As previously stated, structures in the proximity such as the tympanic bones are hypermineralized as well to reduce the acoustic impedance mismatch [2,7] suggesting a local mechanism at the region of the ear to be responsible for the hypermineralization.

Mineralization and mechanical function of bone is linked to the osteocytic environment within the bone, e.g. through secretion of osteocyte-specific proteins such as fibroblast growth factor 23 or sclerostin. Here, we found a similar density of osteocytes in all three ossicles, yet a significantly higher lacunar area in the stapes. Importantly, we detected a very high number of hypermineralized (micropetrotic) osteocyte lacunae in the malleus and incus. This phenomenon was previously detected in aged human bone (femur) [28,29] as well as in human auditory ossicles [13] and seems to go along with a high mineralization of the remaining bone matrix. FTIR analysis revealed almost a four times higher MMR of the whale ossicles (in this case the incus was used) compared to human ossicles and five times higher MMR compared to the same animal's vertebral bone, indicating a local mechanism of hypermineralization. The increased MMR is clearly linked to an increased mineral content with respect to the collagen content, confirming the results of the qBEI analysis. Yet comparing the results from qBEI with those from FTIR analysis, the almost fourfold increase in the MMR via FTIR compared to a lesser increase of mineralization via qBEI can partially be explained by a decreased collagen content in the ossicles. Regarding the CPR, no difference of vertebral bone and human incus was found; however, a significantly higher CPR was detected in the sperm whale's incus. CPR in bone is linked to the mineral age of bone and increases with age by substituting phosphate with carbonate [30]. However, since phosphorous represents a limited factor in aquatic animals as opposed to sufficient calcium in salt water [31], a high CPR can also be the result of low phosphate. Thus we hypothesize the very high CPR in the ossicles of the sperm whale to be owing to an accelerated mineralization at a very young age of the sperm whale to gain a sufficient hearing competence despite limited access to phosphorous.

Compositional differences of bone are reflected by their mechanical behaviour, thus we performed nano-indentation to test for changes linked to compositional differences. We found a 2.45 times higher Young's modulus and three times harder bone in the sperm whale incus compared to human incus as well as significantly lower values for the vertebral bones of the sperm whale. These results clearly suggest the meaning of the hypermineralization and low collagen content of ossicles bone compared to the vertebral body.

Several attempts have been performed to model the ear of the whale as well as to study the sound perception in whales [2,32,33]. Furthermore, middle ear parameters were studied for understanding impedance matching and high-frequency hearing [6,34]. A harder and stiffer bone exhibits a shift towards higher natural-frequencies (ω, as derived from the second derivative of the equation of motion of a simplified body spring system, $\omega = \sqrt{c/m}$; $\omega =$ natural frequency, $c =$ spring constant, thus stiffness of the material, linked to Young's modulus and mineral content, $m =$ mass of a body excited depending on the size). Because the larger scaled ossicles of sperm whales (when compared with other mammals)

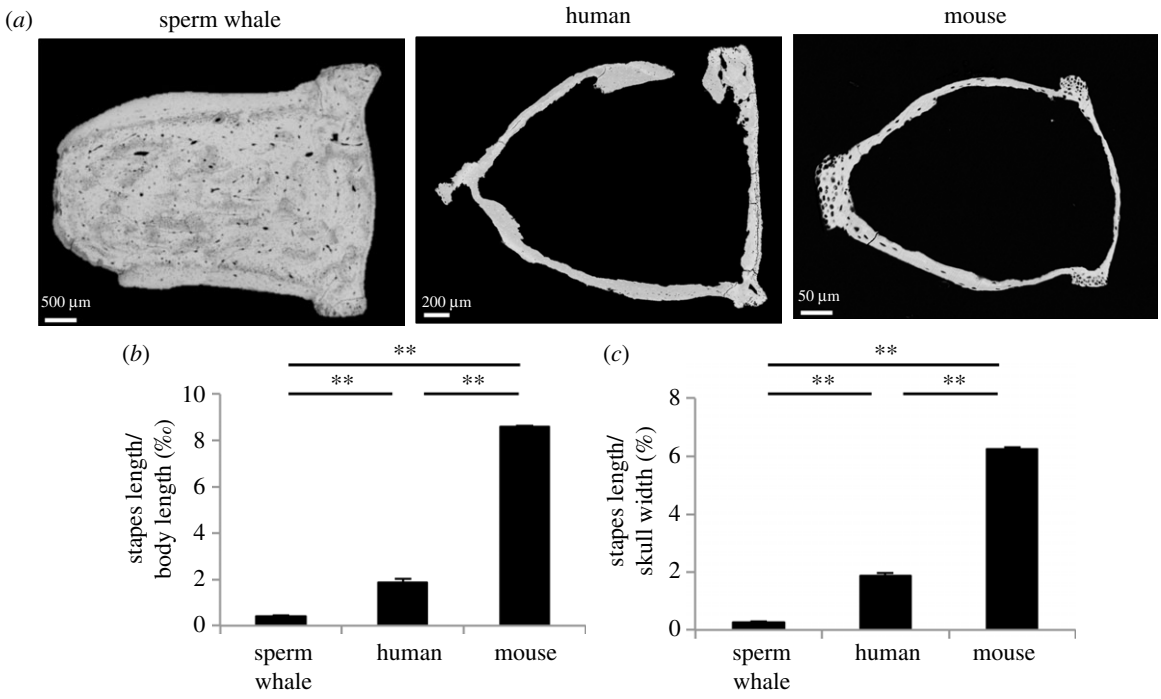

Figure 6. Solid shape and smaller size of the sperm whale stapes. (*a*) No void was detected within the crura of the stapes as opposed to the human and murine stapes (the shape of the human stapes is interrupted owing to the 2D imaging). (*b*) Lower stapes length to body length ratio in sperm whales. (*c*) Stapes length to skull width ratio was equally lower in sperm whales pointing to negative allometry across the species. $^{**}p < 0.001$.

would shift the natural frequencies towards lower values, the increased mineralization of ossicles may compensate this potential natural-frequency shift [6] to avoid interference with the hearing range frequencies and thereby preserving excellent hearing. More specifically, the increased Young's modulus of the ossicles owing to higher mineralization increases the spring constant c, shifting ω towards higher values. This promotes the ideally lossless transmittance of vibrations from the tympanic bone to the oval window and is of paramount importance to the sperm whale because its hearing frequencies reach well above 30 kHz.

In conclusion, we have demonstrated that sperm whale ossicles are functionally hypermineralized bones that exhibit a higher mineralization than the ossicles of other species as well as markedly higher mineralization than their own teeth and vertebral bodies. High mineral and low collagen content render a stiffer and harder material being most suitable to transmit high-frequency sounds through the middle ear. The high mineralization is linked to a high number of hypermineralized osteocyte lacunae. Our results underline the association between high matrix mineralization and hearing capacities, which seem to be an evolutionary conserved or convergent phenomenon.

Ethics. The specimens of the stranded sperm whales were transferred with special documentation of no commercial or trading interests according to the environmental authority of Schleswig-Holstein (Germany) and approved by the Institute for Terrestrial and Aquatic Wildlife Research (ITAW) on behalf of the Schleswig-Holstein Wadden Sea National Park.

Data accessibility. Detailed data are available in the electronic supplementary material.

Authors' contributions. Conceptualization: F.N.S., U.S., R.O., M.A. and T.R.; data curation: F.N.S., M.D. K.M., M.H., U.S., B.B., R.O., M.A. and T.R.; formal analysis: F.N.S., M.D. K.M., M.H., U.S., B.B., R.O., M.A. and T.R.; funding acquisition: n/a; investigation: F.N.S., M.D., K.M., T.A.Y., M.H., U.S., B.B., R.O., M.A. and T.R.; methodology: F.N.S. and T.R.; writing—original draft: F.N.S. and T.R.; writing—review and editing: F.N.S., T.A.Y., U.S., B.B., M.A. and T.R.

Competing interests. The authors have no competing interests.

Funding. B.B. is supported by the German Research Foundation under grant no. BU 2562/3-1.

Acknowledgements. The authors thank all co-workers involved in the recovery and necropsy of the sperm whale carcasses in German waters and appreciate the assistance of the technical staff at the Government-owned Company for Coastal Protection, National Parks and Ocean Protection of Schleswig-Holstein (LKN.SH). Necropsies were funded by the Energy, Agriculture, the Environment, Nature and Digitalization of Schleswig-Holstein, Germany. The authors thank Peter Wohlsein for the support in the preparation of the auditory ossicles, Elke Leicht for the technical assistance and Hinnerk C. Schmidt for his valuable and committed discussion about the vibrational transmission in the middle ear. F.N.S. acknowledges a PhD Scholarship of the Joachim Herz Stiftung in cooperation with the PIER network of University of Hamburg.

References

1. Nummela S, Thewissen JGM, Bajpai S, Hussain T, Kumar K. 2007 Sound transmission in archaic and modern whales: anatomical adaptations for underwater hearing. *Anat. Rec. (Hoboken)* **290**, 716–733. (doi:10.1002/ar.20528)
2. Hemilä S, Nummela S, Reuter T. 1999 A model of the odontocete middle ear. *Hear. Res.* **133**, 82–97. (doi:10.1016/S0378-5955(99)00055-6)
3. Ketten DR. 1997 Structure and function in whale ears. *Bioacoustics* **8**, 103–135. (doi:10.1080/09524622.1997.9753356)
4. Cranford TW, Krysl P. 2015 Fin whale sound reception mechanisms: skull vibration enables low-frequency hearing. *PLoS ONE* **10**, e0116222. (doi:10.1371/journal.pone.0116222)
5. Cranford TW, Krysl P, Amundin M. 2010 A new acoustic portal into the odontocete ear and vibrational analysis

of the tympanoperiotic complex. *PLoS ONE* **5**, e11927. (doi:10.1371/journal.pone.0011927)

6. Nummela S, Wägar T, Hemilä S, Reuter T. 1999 Scaling of the cetacean middle ear. *Hear. Res.* **133**, 71–81. (doi:10.1016/S0378-5955(99)00054-4)
7. Currey JD. 1979 Mechanical properties of bone tissues with greatly differing functions. *J. Biomech.* **12**, 313–319. (doi:10.1016/0021-9290(79)90073-3)
8. Tubelli AA, Zosuls A, Ketten DR, Mountain DC. 2014 Elastic modulus of cetacean auditory ossicles. *Anat. Rec. (Hoboken)* **297**, 892–900. (doi:10.1002/ar.22896).
9. Madsen PT, Johnson M, Miller PJ, Aguilar Soto N, Lynch J, Tyack P. 2006 Quantitative measures of air-gun pulses recorded on sperm whales (*Physeter macrocephalus*) using acoustic tags during controlled exposure experiments. *J. Acoust. Soc. Am.* **120**, 2366–2379. (doi:10.1121/1.2229287)
10. Wartzok D, Ketten DR. 1999 Marine mammal sensory systems. In *Biology of marine mammals* (eds J Reynolds, S Rommel), pp. 117–175. Washington, DC: Smithsonian Institution Press.
11. Hemilä S, Nummela S, Reuter T. 2001 Modeling whale audiograms: effects of bone mass on high-frequency hearing. *Hear. Res.* **151**, 221–226. (doi:10.1016/S0378-5955(00)00232-X)
12. Palumbo C, Cavani F, Sena P, Benincasa M, Ferretti M. 2012 Osteocyte apoptosis and absence of bone remodeling in human auditory ossicles and scleral ossicles of lower vertebrates: a mere coincidence or linked processes? *Calcif. Tissue Int.* **90**, 211–218. (doi:10.1007/s00223-012-9569-6)
13. Rolvien T *et al.* 2018 Early bone tissue aging in human auditory ossicles is accompanied by excessive hypermineralization, osteocyte death and micropetrosis. *Sci. Rep.* **8**, 1920. (doi:10.1038/s41598-018-19803-2)
14. Kanzaki S, Ito M, Takada Y, Ogawa K, Matsuo K. 2006 Resorption of auditory ossicles and hearing loss in mice lacking osteoprotegerin. *Bone* **39**, 414–419. (doi:10.1016/j.bone.2006.01.155)
15. Lysaght AC, Yuan Q, Fan Y, Kalwani N, Caruso P, Cunnane M, Lanske B, Stankovic KM. 2014 FGF23 deficiency leads to mixed hearing loss and middle ear malformation in mice. *PLoS ONE* **9**, e107681. (doi:10.1371/journal.pone.0107681)
16. Rolvien T, Hahn M, Siebert U, Puschel K, Wilke HJ, Busse B, Amling M, Oheim R. 2017 Vertebral bone microarchitecture and osteocyte characteristics of three toothed whale species with varying diving behaviour. *Sci. Rep.* **7**, 1604. (doi:10.1038/s41598-017-01926-7)
17. Schnitzler JG, Frederich B, Fruchtnicht S, Schaffeld T, Baltzer J, Ruser A, Siebert U. 2017 Size and shape variations of the bony components of sperm whale cochleae. *Sci. Rep.* **7**, 46734. (doi:10.1038/srep46734)
18. Simon MJ *et al.* 2014 High fluoride and low calcium levels in drinking water is associated with low bone mass, reduced bone quality and fragility fractures in sheep. *Osteoporos. Int.* **25**, 1891–1903. (doi:10.1007/s00198-014-2707-4)
19. Yorgan TA, Peters S, Jeschke A, Benisch P, Jakob F, Amling M, Schinke T. 2015 The anti-osteoanabolic function of sclerostin is blunted in mice carrying a high bone mass mutation of Lrp5. *J. Bone Miner. Res.* **30**, 1175–1183. (doi:10.1002/jbmr.2461)
20. Priemel M *et al.* 2010 Bone mineralization defects and vitamin D deficiency: histomorphometric analysis of iliac crest bone biopsies and circulating 25-hydroxyvitamin D in 675 patients. *J. Bone Miner. Res.* **25**, 305–312. (doi:10.1359/jbmr.090728)
21. Hahn M, Vogel M, Delling G. 1991 Undecalcified preparation of bone tissue: report of technical experience and development of new methods. *Virchows Arch. A Pathol. Anat. Histopathol.* **418**, 1–7. (doi:10.1007/BF01600238)
22. Roschger P, Paschalis EP, Fratzl P, Klaushofer K. 2008 Bone mineralization density distribution in health and disease. *Bone* **42**, 456–466. (doi:10.1016/j.bone.2007.10.021)
23. Koehne T, Vettorazzi E, Kusters N, Luneburg R, Kahl-Nieke B, Puschel K, Amling M, Busse B. 2014 Trends in trabecular architecture and bone mineral density distribution in 152 individuals aged 30–90 years. *Bone* **66**, 31–38. (doi:10.1016/j.bone.2014.05.010)
24. Milovanovic P, vom Scheidt A, Mletzko K, Sarau G, Püschel K, Djuric M, Amling M, Christiansen S, Busse B. 2018 Bone tissue aging affects mineralization of cement lines. *Bone* **110**, 187–193. (doi:10.1016/j.bone.2018.02.004)
25. Roschger P, Fratzl P, Eschberger J, Klaushofer K. 1998 Validation of quantitative backscattered electron imaging for the measurement of mineral density distribution in human bone biopsies. *Bone* **23**, 319–326. (doi:10.1016/S8756-3282(98)00112-4)
26. Seeman E. 2008 Chapter 1 - modeling and remodeling: the cellular machinery responsible for the gain and loss of bone's material and structural strength. In *Principles of bone biology (third edition)* (eds JP Bilezikian, LG Raisz, TJ Martin), pp. 1–28. San Diego, CA: Academic Press.
27. Giraud-Sauveur D. 1969 Recherches biophysiques sur les osselets des cétacés. *Mammalia* **33**, 285–340. (doi:10.1515/mamm.1969.33.2.285)
28. Busse B, Djonic D, Milovanovic P, Hahn M, Puschel K, Ritchie RO, Djuric M, Amling M. 2010 Decrease in the osteocyte lacunar density accompanied by hypermineralized lacunar occlusion reveals failure and delay of remodeling in aged human bone. *Aging Cell* **9**, 1065–1075. (doi:10.1111/j.1474-9726.2010.00633.x)
29. Milovanovic P *et al.* 2017 The formation of calcified nanospherites during micropetrosis represents a unique mineralization mechanism in aged human bone. *Small* **13**, 1602215. (doi:10.1002/smll.201602215)
30. Boskey A, Pleshko Camacho N. 2007 FT-IR imaging of native and tissue-engineered bone and cartilage. *Biomaterials* **28**, 2465–2478. (doi:10.1016/j.biomaterials.2006.11.043)
31. Rolvien T *et al.* 2016 How the European eel (*Anguilla anguilla*) loses its skeletal framework across lifetime. *Proc. R. Soc. B* **283**, 20161550. (doi:10.1098/rspb.2016.1550)
32. Goold JC, Jones SE. 1995 Time and frequency domain characteristics of sperm whale clicks. *J. Acoust. Soc. Am.* **98**, 1279–1291. (doi:10.1121/1.413465)
33. Madsen PT, Payne R, Kristiansen NU, Wahlberg M, Kerr I, Møhl B. 2002 Sperm whale sound production studied with ultrasound time/depth-recording tags. *J. Exp. Biol.* **205**, 1899–1906.
34. Hemilä S, Nummela S, Reuter T. 1995 What middle ear parameters tell about impedance matching and high frequency hearing. *Hear. Res.* **85**, 31–44. (doi:10.1016/0378-5955(95)00031-X)